



Mathematisch-Naturwissenschaftliche Fakultät

Giovanna Rizzo | Salvatore Laurita | Uwe Altenberger

# The Timpa delle Murge ophiolitic gabbros, southern Apennines

Insights from petrology and geochemistry and consequences to the geodynamic setting

Suggested citation referring to the original publication:

Periodico di Mineralogia 87 (2018) 5-20

DOI <https://doi.org/10.2451/2018PM741>

ISSN (print) 0369-8963

ISSN (online) 0369-8963

Postprint archived at the Institutional Repository of the Potsdam University in:

Postprints der Universität Potsdam

Mathematisch-Naturwissenschaftliche Reihe ; 1002

ISSN 1866-8372

<https://nbn-resolving.org/urn:nbn:de:kobv:517-opus4-459928>

DOI <https://doi.org/10.25932/publishup-45992>





## The Timpa delle Murge ophiolitic gabbros, southern Apennines: insights from petrology and geochemistry and consequences to the geodynamic setting

Giovanna Rizzo <sup>a,\*</sup>, Salvatore Laurita <sup>a</sup>, Uwe Altenberger <sup>b</sup>

<sup>a</sup> Department of Sciences, University of Basilicata, Campus di Macchia Romana, Via dell'Ateneo Lucano, 10, 85100 Potenza, Italy

<sup>b</sup> Institute of Earth and Environmental Science, University of Potsdam, Germany

### ARTICLE INFO

Submitted: July 2017

Accepted: October 2017

Available on line: November 2017

\* Corresponding author:  
giovanna.rizzo@unibas.it

DOI: 10.2451/2018PM741

How to cite this article:  
Rizzo G. et al. (2018)  
Period. Mineral. 87, 5-20

### ABSTRACT

The Timpa delle Murge ophiolite in the North Calabrian Unit is part of the Liguride Complex (southern Apennines). The study is concentrated on the gabbroic part of the ophiolite of the Pollino area. They preserve the high-grade ocean floor metamorphic and locally developed flaser textures under ocean floor conditions. The primary magmatic assemblages are clinopyroxene, plagioclase, and opaques. Brown hornblende is a late magmatic phase. Green hornblende, actinolite, albite, chlorite and epidote display metamorphic recrystallization under lower amphibolite facies conditions, followed by greenschist facies.

The gabbros show subalkaline near to alkaline character with a tendency to a more calcalkaline trend. The normalization to primitive mantle and mid-ocean ridge basalt (N-MORB) compositions indicates a considerable depletion in Nb, P, Zr and Ti and an enrichment in Ba, Rb, K, Sr and Eu. This points to a mantle source, which is not compatible with a "normal" mid-ocean ridge situation. Rather, the gabbros are generated from a N-MORB-like melt with a strong crustal component, which was influenced by subduction related fluids and episodic melting during mid-ocean-ridge processes.

Plausible geodynamic settings of the Timpa delle Murge gabbros are oceanic back-arc positions with embryonic MORB-activities. Similar slab contaminated magmatism is also known from the early stage of island arc formation in supra-subduction zone environments like the Izu-Bonin-Mariana island arc.

Keywords: Southern Apennines; Liguride Complex; North Calabrian Unit; ophiolite; gabbros.

### INTRODUCTION

Ophiolites give important information about the composition of the fossil oceanic lithosphere and upper mantle. They give an insight into the processes of partial melting and the location of mantle formation, e.g. mid-ocean ridge vs back arc basin origin and lithospheric versus asthenospheric mantle. Therefore, they are considered to be significant for the reconstruction of the paleotectonic evolution of orogenic belts.

Ophiolites can be classified to the first order as subduction-related and subduction-unrelated types (Dilek and Furnes, 2014). Subduction-related ophiolites include suprasubduction zone (SSZ) and volcanic arc (VA) ophiolites. The SSZ type ophiolites formed in subduction-initiation (forearc) and backarc basin settings. Subduction-unrelated types include continental margin (CM), mid-ocean ridge (MOR), and plume-type (P) ophiolites (Pearce, 2014).

The ophiolitic sequences of the southern Apennines are remnants of the Jurassic western Tethys realms (Figure 1 a,b,c). The ophiolite is part of the Liguride Complex (Ogniben, 1969), which represents the upper structural unit of the southern Apennines. It includes sequences characterized by high pressure/low temperature metamorphic overprint: the Frido Unit (Vezzani, 1969; 1970; Lanzafame et al., 1979; Spadea, 1982; Sansone and Rizzo, 2012; Sansone et al., 2012 a,b) and sequences lacking of an orogenic metamorphism: the North Calabrian Unit (Bonardi et al., 1988).

In this study we present new geochemical analyses of the gabbro unit of the ophiolite of the North Calabrian Unit (Pollino Massif, Italy, Figure 1a). We show new results and give new models for the mantle source generating the melts and for the geodynamic setting, as well as for later melt modifying processes. We compare the ophiolite of the North Calabria Unit with the other ophiolitic complexes as Albanide-Hellenide systems and the Internal Ligurides (Vara Unit). These new results may be important for the geodynamic evolution of the Mediterranean area.

**GEOLOGICAL SETTING**

The Southern Apennine Chain is a fold and thrust belt as resulted from the convergence between African and European plates (upper Oligocene-Quaternary) (Patacca and Scandone, 2007 and references therein) and the simultaneous rollback of the SE-directed Ionian subduction (Gueguen et al., 1998; Cello and Mazzoli, 1999; Doglioni et al., 1999). In the Southern Apennine, the accretionary wedge is related to the Oligocene northward subduction of an Alpine Tethys sector as Stampfli et al. (2002) or western Thetys sector as Bracciali et al. (2007) supposed.

The Calabrian-Lucanian Apennine is a sector of the southern Apennines at the Lucania-Calabria border zone along the northeast of the Pollino chain (Monaco et al., 1995). This sector includes allochthonous parts of the Liguride Complex (Schiattarella, 1996; Giano et al., 2014; Giano and Giannandrea, 2014). They are formed in the Late Cretaceous-Oligocene times (Knott, 1994) after NW-directed subduction of the oceanic and thinned continental lithosphere of the Alpine Tethys (Ciarcia et al.,

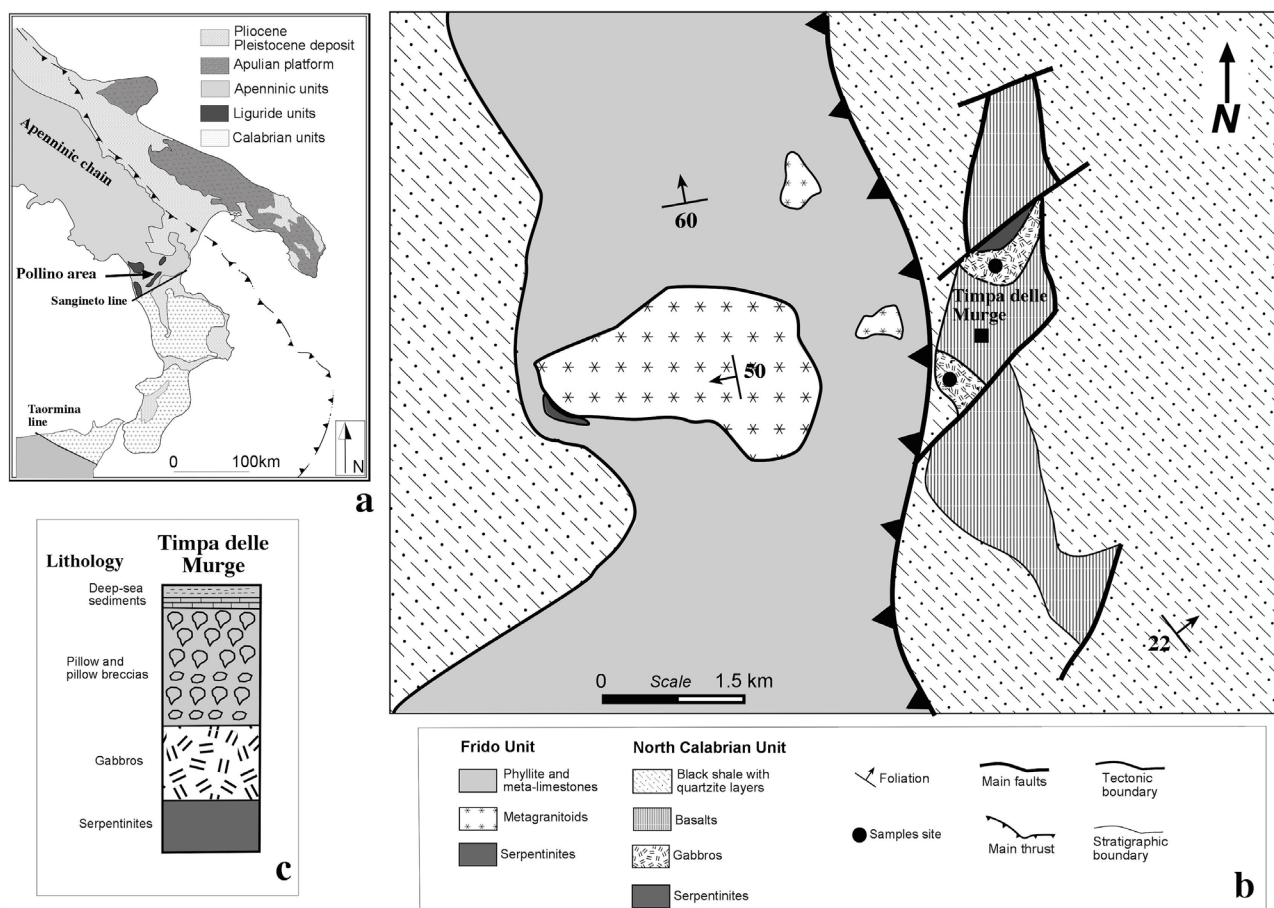


Figure 1. a) Tethyan Ophiolites of Southern Apennines; b) simplified geological map of the studied area; c) schematic column of the sample area (isn't in scale).

2012). The Calabrian-Lucanian Apennine was originally interposed between a northern continental margin (Turco et al., 2012) and the Adria block, of African affinity, to the south (Vitale et al., 2013).

The Liguride Complex includes bodies of oceanic and continental crust (Vezzani, 1969, Laurita et al., 2014) as well as sedimentary sequences (Upper Jurassic to Upper Oligocene, Monaco and Tortorici, 1995). More in particular, the Liguride Complex constituted, from bottom to top by the North Calabrian Unit, the Frido Unit, and the Crystalline metamorphic Units (Di Leo et al., 2005). The North Calabrian Unit is composed of the Crete Nere Formation, the Saraceno Formation and the Albidona Formation (Di Leo et al., 2005).

The North Calabrian Unit is a broken formation that, tectonically dismembered into several thrust sheets, is made up of a succession of pelitic matrix containing blocks of ophiolites, pelagic sediments, turbiditic sequences and very rare andesites and dacites (Tortorici et al., 2009). This unit has been affected by oceanic alteration (Sansone et al., 2012 a,b) and is lacking any orogenic metamorphism.

The Frido Unit consists of low-grade phyllites, calcschists, and metalimestones with associated ophiolites (Rizzo et al., 2016). Slivers of continental crust (Spadea, 1982; Knott, 1987, 1994; Monaco et al., 1995; Monaco and Tortorici, 1995; Tortorici et al., 2009) occur as a thrust fault delimiting the upper portion of this unit from a lower portion (Laurita et al., 2014).

#### **OPHIOLITES OF THE SOUTHERN APENNINES**

Ophiolites of the Southern Apennines (Figure 1) are extensively exposed in the northeastern slope of the Pollino Ridge (Vezzani, 1969; Bonardi et al., 2009; Monaco and Tortorici, 1995; Vitale et al., 2013; Sansone et al., 2011). They occur in the high-pressure (HP) metamorphic Frido Unit as well as in the low grade North Calabrian Unit.

Ophiolite bodies of the blueschist-facies metamorphic Frido Unit consist of serpentinites derived from a lherzolitic and subordinately harzburgitic mantle (Lanzafame et al., 1979; Spadea, 1982; Beccaluva et al., 1982; Sansone et al., 2011; Sansone et al., 2012 a,b; Vitale et al., 2013; Dichicco et al., 2015; Dichicco et al., 2017) minor metagabbros, metabasalts, diabases and their respective sedimentary cover (Vezzani, 1970; Spadea, 1982, 1994).

Ophiolites of the North Calabrian Unit (Timpa delle Murge, Timpa di Pietrasasso sequence, (Figure 1 a,b,c), on which this work is concentrated do not exhibit any subduction related high-pressure metamorphism (Lanzafame et al., 1978; Bonardi et al., 1988). They are composed of scarce Mg-gabbro cumulates (Spadea, 1979) and stratigraphically overlain by pillow lavas pillow breccias, hyaloclastites, diabases. The sedimentary

cover consists of siliceous shales, radiolarian cherts, and limestones (Lanzafame et al., 1979).

The gabbros of the Frido Unit and the North Calabrian Unit are only a small part of the ophiolites from the Calabria-Lucania area and occur as bodies not exceeding one km<sup>3</sup> in volume (Beccaluva et al., 1982). They consist mainly of saussuritized plagioclase, olivine and relics of clinopyroxene (diopside according to Beccaluva et al., 1982; or diallage according to Lanzafame et al., 1978). The occurrence of brown hornblende suggests a recrystallization under amphibolite followed by greenschist facies conditions (Beccaluva et al., 1982).

The nearby diabases show intersertale, subophitic textures (Lanzafame et al., 1978). Metamorphism of the gabbros and diabases is characterized by prehnite-pumpellyite facies to greenschist facies mineral assemblages. The oceanic metamorphic evolution is characterized by albite, chlorite, tremolitic hornblende, white mica and epidote. Pillows and pillow breccias preserve their original structure and minerals. The prevalent basaltic rocks have intersertal structure, while porphyric rocks are rare (Lanzafame et al., 1978, 1979; Bonardi et al., 1988).

#### **OPHIOLITES OF THE ALBANIDE AND HELLENIDE**

Ophiolites of the Albanide-Hellenide include mid-ocean ridge basalt (MORB) associations in the western Mirdita sector and supra-subduction zone (SSZ) complexes, with prevalent island arc tholeiitic (IAT) and minor boninitic affinities in the eastern part of the belt (i.e. eastern Mirdita, Pindos, Vourinos) (Beccaluva et al., 2005). These ophiolites formed in an intraoceanic subduction setting located near an active mid-ocean spreading ridge (Bebien et al., 2000; Insergueix-Filippi et al., 2000).

Some authors also considered a model where the Albanide-Hellenide ophiolites formed in a back-arc spreading system oblique to a west-dipping subduction zone (Hoeck et al., 2002).

#### **OPHIOLITES OF THE INTERNAL LIGURIDES**

The Internal Ligurides ophiolites is a remnant of the oceanic lithosphere of the Jurassic Ligurian Tethys, and consists of depleted mantle peridotites (Rampone et al., 1996, 1997, 2008, 2009; Rampone and Hofmann, 2012) intruded by large-scale MOR-type gabbroic sequences (Principi et al., 2004; Menna, 2009; Sanfilippo and Tribuzio, 2013) and covered by pillow lavas and ophiolitic breccias. The structural and compositional characteristics are similar to oceanic lithosphere from slow and ultra-slow spreading ridges (Lagabrielle and Cannat, 1990; Tribuzio et al., 1995, 1999, 2004; Sanfilippo and Tribuzio, 2011; Alt et al., 2012; Schwarzenbach et al., 2012).

### SAMPLING AND ANALYTICAL METHODS

Seven samples of gabbros of the North-Calabrian Unit were collected at Timpa delle Murge. They were examined petrographically under optical microscopy and scanning electron microscopy coupled with EDX. This analysis was performed by using a Philips (XL30 ESEM) instruments, operated at 20 KV acceleration voltage and 15 nA beam current.

Bulk analyses were carried out by XRF and ICP-MS (Table 1). Major elements were measured at the Dipartimento di Biologia, Università della Calabria (Arcavacata di Rende, Cosenza, Italy) by XRF on powder pellets, using XRF BRUKER S8 TIGER and following the matrix correction methods by Franzini et al. (1972, 1975), and Leoni and Saitta (1976). Average errors for trace elements were less than 5% except for those elements lower than 10 ppm (5-10%). The estimated precision and accuracy for trace element determinations are better than 5%, except for those elements having a concentration of lower than 10 ppm (10-15%). Total loss on ignition was gravimetrically estimated by overnight heating at 950 °C. The standards used to calibrate XRF analyses were: AGVB1, AGVB2, BCRB1, BCRB2, BR, DRBN, GA, GSPB1, GSPB2, NIMBG. The concentration of the rare earth elements (REE) and other trace elements (Sc, V, Ba, Sr, Y, Zr, Cr, Co, Ni, Cu, Ga, Ge, Rb) were obtained at the Ancaster Activation Laboratories, Canada, by ICP-MS. Average errors for these different elements range from 5 to 20%.

### PETROGRAPHY

The gabbros of the ophiolitic suite are medium to coarse grained and of dark to light green color. They are

generally composed of 40–60 vol% plagioclase and 30–50 vol% clinopyroxene. Amphiboles (brown amphiboles, green amphiboles and actinolite) are minor constituents (1-10 vol%). The gabbros have usually a cumulate texture and they don't show any evidence of shape- or lattice-preferred orientation. The common occurrence of large subhedral clinopyroxenes (Figure 2a) indicates that these are the dominant cumulate phase, with plagioclase both as cumulus and as intercumulus.

In addition to the primary magmatic paragenesis clinopyroxene, plagioclase (pl 1) (Figure 2b), other mineralogical phases (green hornblende, actinolite, chlorite, epidote, plagioclase (pl 2), quartz and white mica and accessory opaque minerals) are formed to lower amphibolite or upper greenschist facies (oceanic) metamorphic minerals. Undeformed coronitic rims of brown hornblende are found around clinopyroxene, suggesting a late magmatic crystallization deriving from alteration of clinopyroxene due to interaction of gabbros with seawater-derived hydrothermal fluids.

Subhedral prisms of plagioclase (grain size of 0.04-0.07 mm) often show deformation twins in addition to growth twins. This reveals, that the plagioclase experienced the activation of intracrystalline deformation under high-temperature (metamorphic) conditions. The analyses of the anorthite content shows  $An > 50$ . However structural and chemical analyses indicate a retrogression to oligoclase ( $An_{12-20}$ , Table 2) and more often to albite ( $An_{5-9}$ , Table 2). Crystals of clinopyroxene (grain size of 0.03-0.07 mm) are subhedral to euhedral, pleochroic from pale-brown-green, and are zoned (Figure 2c, Table 3). Some crystals show exsolution lamellae of orthopyroxene or exsolved iron oxides along cleavage

Table 1. Chemical composition of the analyzed gabbros.

wt%	GI1	GI2	GI3	GI4	GI5	GI6	GI7
SiO <sub>2</sub>	51.56	51.14	49.13	50.99	49.45	50	49
TiO <sub>2</sub>	0.243	0.324	0.269	0.218	0.254	0.252	0.26
Al <sub>2</sub> O <sub>3</sub>	15.01	19.54	18.48	15.2	17.69	17	18
Fe <sub>2</sub> O <sub>3</sub> (T)	4.79	3.77	5.07	5.36	4.75	4.7	5.06
MnO	0.117	0.102	0.127	0.125	0.11	0.1	0.1
MgO	10.24	6.38	8.07	11.58	8.09	8.05	8.06
CaO	9.7	9.63	9.62	8.56	9.66	9.7	9.6
Na <sub>2</sub> O	3.01	3.51	3.57	3.16	3.4	3.3	3.5
K <sub>2</sub> O	1.18	1.69	0.74	0.93	0.87	0.85	0.8
P <sub>2</sub> O <sub>5</sub>	0.02	0.02	0.0001	0.0001	0.0001	0.0001	0.0001
LOI	3.77	3.81	4.52		4.11	4.42	4.4
Total	99.63	99.92	99.58	100.2	98.68	98.35	98.68

Table 1. ... Continued

ppm	GI1	GI2	GI3	GI4	GI5	GI6	GI7
Sc	40	28	31	36	32	32	32
Be	<1	<1	<1	<1	<1	<1	<1
V	146	124	130	128	131	131	129
Ba	56	125	155	39	112	112	120
Sr	116	175	166	164	136	136	140
Y	6	7	6	6	6	6	6
Zr	6	16	9	5	8	8	9
Cr	430	130	110	420	130	130	129
Co	32	20	29	38	31	31	30
Ni	150	50	80	180	90	90	95
Cu	20	50	30	< 10	180	180	160
Zn	<30	<30	<30	<30	<30	<30	<30
Ga	9	12	12	9	11	11	10
Ge	1	1	2	1	2	2	2
As	<5	<5	<5	<5	<5	<5	<5
Rb	7	11	5	6	5	5	6
Nb	<1	<1	<1	<1	<1	<1	<1
Mo	<2	<2	<2	<2	<2	<2	<2
Ag	<0.5	<0.5	<0.5	<0.5	<0.5	<0.5	<0.5
In	<0.2	<0.2	<0.2	<0.2	<0.2	<0.2	<0.2
Sn	<1	6	<1	<1	<1	<1	<1
Sb	<0.5	<0.5	<0.5	<0.5	<0.5	<0.5	<0.5
Cs	0.7	1.2	<0.5	0.5	<0.5	<0.5	<0.5
La	0.5	0.9	0.6	0.4	0.5	0.5	0.6
Ce	1.1	2.2	1.5	0.9	1.3	1.3	1.4
Pr	0.17	0.33	0.23	0.17	0.22	0.22	0.24
Nd	1.3	1.9	1.6	1.1	1.2	1.2	1.4
Sm	0.5	0.7	0.6	0.4	0.5	0.5	0.6
Eu	0.25	0.47	0.46	0.35	0.38	0.38	0.4
Gd	0.8	0.9	0.9	0.7	0.8	0.8	0.8
Tb	0.2	0.2	0.2	0.1	0.2	0.2	0.2
Dy	1.1	1.3	1.1	0.9	1.1	1	1.1
Ho	0.2	0.3	0.2	0.2	0.2	0.2	0.3
Er	0.7	0.8	0.7	0.6	0.7	0.7	0.8
Tm	0.11	0.12	0.11	0.09	0.11	0.11	0.1
Yb	0.7	0.8	0.7	0.6	0.7	0.7	0.8
Lu	0.1	0.12	0.1	0.1	0.1	0.1	0.15
Hf	<0.2	0.3	0.2	<0.2	0.2	0.2	0.3
Ta	<0.1	<0.1	<0.1	<0.1	<0.1	<0.1	<0.1
W	2	1	1	<1	<1	<1	<1
Tl	0.1	<0.1	<0.1	<0.1	<0.1	<0.1	<0.1
Pb	<5	<5	<5	<5	<5	<5	<5



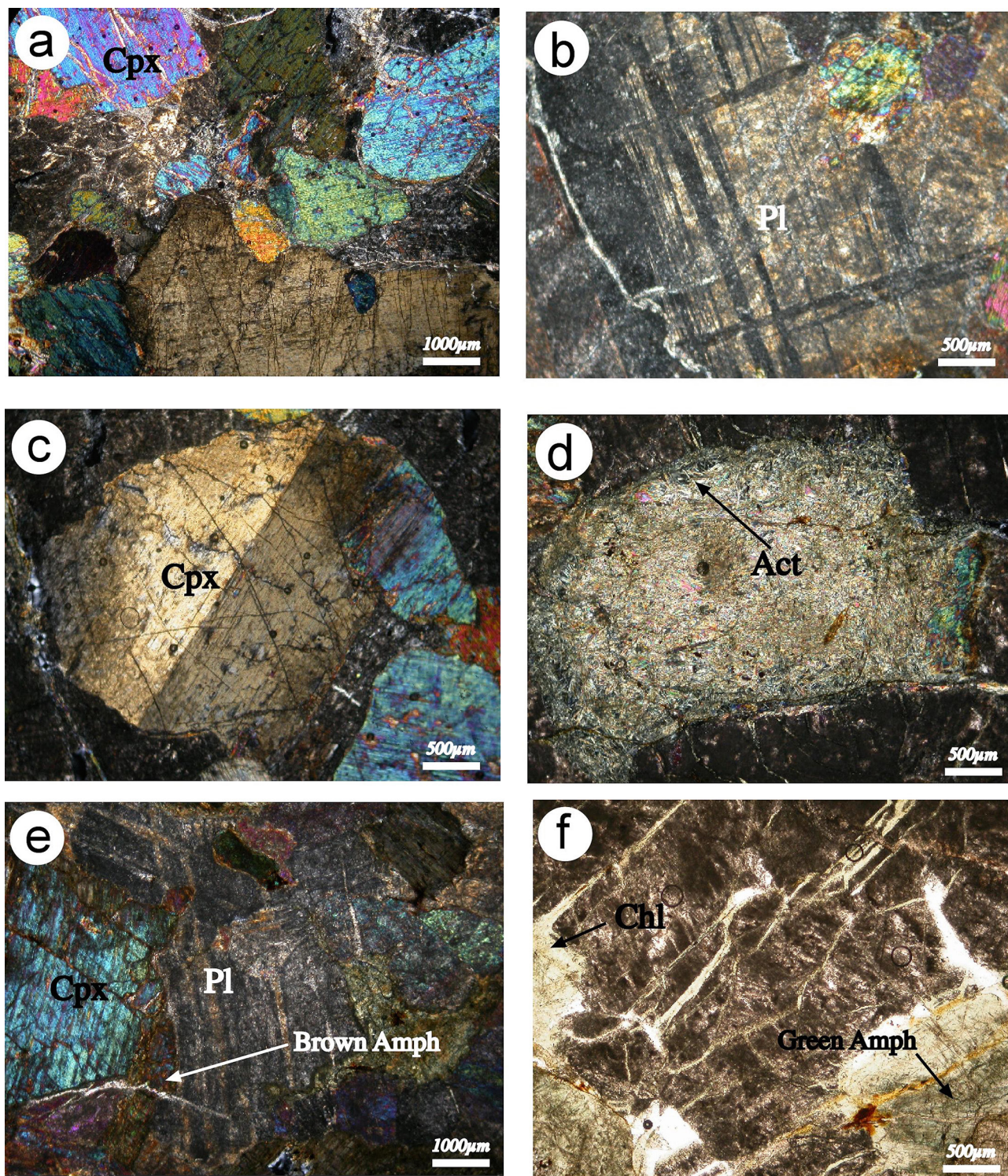


Figure 2. Microphotographs of thin section of the studied gabbros. a) igneous texture and coarse grain size; b) large subhedral plagioclase with deformation twins, with minor sericitization along grain boundaries; c) common habit of clinopyroxene with thin orthopyroxene exsolution lamellae along cleavage plane; d) interstitial actinolite in zone of alteration; e) minor brown hornblende occurs often forming undeformed coronitic rim around clinopyroxene; f) green amphiboles and aggregates of chlorite, representing the hydrothermal/metamorphic stage. Cpx=clinopyroxene; Pl=plagioclase; Act=actinolite; Chl=chlorite.



Table 2. Chemical composition of plagioclase.

wt%	GI2.1	GI3.1	GI3.2	GI2.2
SiO <sub>2</sub>	70.29	71.18	72.48	72.60
Al <sub>2</sub> O <sub>3</sub>	19.41	18.64	18.00	18.19
FeO	0.00	0.00	0.13	0.00
MnO	0.00	0.012	0.00	0.00
CaO	2.06	0.69	0.33	0.52
Na <sub>2</sub> O	8.29	9.13	9.14	8.67
K <sub>2</sub> O	0.00	0.10	0.00	0.02
Total	100.05	99.75	100.08	100.00
Si <sup>4+</sup>	3.04	3.08	3.12	3.12
Al <sup>3+</sup>	0.99	0.95	0.91	0.92
Fe <sup>2+</sup>	0.00	0.00	0.001	0.00
Mn <sup>2+</sup>	0.00	0.001	0.001	0.00
Ca <sup>2+</sup>	0.10	0.03	0.02	0.02
Na	0.69	0.77	0.76	0.72
K	0.00	0.01	0.001	0.00
Total	4.82	4.83	4.81	4.78
Ab	87.93	95.33	98.04	96.65
An	12.07	3.98	1.96	3.20
Or	0.00	0.69	0.00	0.15

planes. Pleochroic yellow to brown amphibole (Figure 2e) occurs subhedral, often forming undeformed coronitic rim around clinopyroxene. Clinopyroxene is replaced by green, subhedral hornblende, indicative of hydrothermal alteration at late magmatic or amphibolite to upper greenschist facies conditions. In addition, clinopyroxene shows commonly rims of actinolite or chlorite (Figure 2d, Table 4, Table 5). Colorless to pale green actinolite (Figure 2f) occurs as prismatic crystals or fibrous aggregates. Chlorite overgrows clinopyroxene or replaces amphibole or forms fan-felt radiated aggregates. Epidote crystals have a pale brownish color and subhedral habit. White mica forms pseudomorphs to plagioclase crystals. Opaque minerals are present as accessory phase, they occur as inclusion in clinopyroxene and actinolite crystals. Sometimes opaque minerals show rims of Fe-hydroxide. Polymineralic veins composed of quartz, plagioclase, chlorite, and white mica cut the gabbros.

#### GEOCHEMISTRY

In addition to their modal composition, the total alkalis/SiO<sub>2</sub> ratios (according to Le Bas et al., 1986) classifies

the samples as gabbros (Table 1, Figure 3). These ratios indicate a subalkaline near to alkaline character. Nevertheless the K<sub>2</sub>O concentrations are mostly below 1.0 wt%. Cr/SiO<sub>2</sub> ratios (according to Middlemost, 1975) reveal a tholeiitic trend, although two samples show a more calc-alkaline trend. All samples have normative olivine, hypersthene and diopside in varying percentage. The samples do not contain neither normative or modal quartz.

The investigated gabbros are characterized by varying but high MgO concentrations of 6.38 to 11.60 wt% with mg#=61-69 [mg#=100Mg/(Mg+Fetot)], Cr concentrations mostly between ca. 130 and 430 ppm, and Ni between ca. 50 and 200 ppm. Therefore, the gabbros represent variable but only weakly fractionated melts of basaltic composition. The samples contain remarkable low concentrations of a few trace elements: only two samples have P<sub>2</sub>O<sub>5</sub> above the detection limit (0.01wt%), Nb and Ta, are below detection limit (1.0 and 0.1 ppm), as well as Th and Pb. TiO<sub>2</sub> concentrations are below 0.25 wt%. Also K<sub>2</sub>O is low with 5 of 7 samples lower than 1.0 wt%. The total amount of rare earth elements (REE) is

Table 3. Chemical composition of clinopyroxenes.

wt%	GI2.1	GI2.4	GI3.2.1	GI3.2.2	GI3.2.3	GI2.1.1
	core	core	core	rim	rim	core
SiO <sub>2</sub>	53.28	53.70	53.73	53.67	54.00	54.00
TiO <sub>2</sub>	0.60	0.54	0.69	0.59	0.58	0.57
Al <sub>2</sub> O <sub>3</sub>	2.42	2.43	2.20	2.02	2.00	2.25
Cr <sub>2</sub> O <sub>3</sub>	0.23	0.17	0.33	0.10	0.01	0.19
FeO	6.63	6.53	6.63	6.84	6.30	6.33
MnO	0.20	0.36	0.11	0.28	0.19	0.24
MgO	13.25	13.43	13.77	13.95	13.80	13.73
CaO	23.20	22.55	22.35	22.00	22.68	22.29
Na <sub>2</sub> O	0.21	0.29	0.21	0.21	0.23	0.24
Total	100.02	100.00	100.02	99.66	99.79	99.84
Si	1.96	1.97	1.97	1.98	1.99	1.98
Ti	0.02	0.01	0.02	0.02	0.02	0.02
Al	0.11	0.11	0.10	0.09	0.09	0.10
Cr	0.01	0.00	0.01	0.00	0.00	0.01
Fe <sup>3+</sup>	0.03	0.03	0.03	0.02	0.02	0.01
Mg	0.73	0.74	0.75	0.77	0.76	0.75
Ca	0.92	0.89	0.88	0.87	0.89	0.88
Mn	0.01	0.01	0.00	0.01	0.01	0.01
Fe <sup>2+</sup>	0.17	0.17	0.17	0.19	0.18	0.19
Na	0.01	0.02	0.01	0.02	0.02	0.02
Total	3.96	3.95	3.95	3.96	3.95	3.95
Mg	39.45	40.43	40.98	41.62	41.08	40.98
SFe	10.81	10.92	10.92	11.35	10.81	10.92
Ca	49.73	48.63	40.08	47.03	48.10	48.08
mg*	66.64	67.28	68.71	67.09	68.65	68.44

quite low, too and below 11ppm. In order to evaluate melt generating and modifying processes in a qualitative way, the compositions of the gabbros have been normalized to chondrite (Figure 3) and primitive mantle (PRIMA; Figure 4) and compared to PRIMA-normalized N-MORB. The chondrite-normalized values (Figure 4) and patterns show a positive slope from light to heavy rare earth elements as pointed out by a  $La_n/Sm_n$  and  $La_n/Yb_n$  ratio below 0.65 and 0.6, except sample 2 with 0.8 and 0.76. However, Eu shows a significant positive anomaly with  $Eu/Eu^*$  between 1.2 and 2.

The normalization to primitive mantle composition (Figure 4) indicates a significant depletion in Nb, P, Zr and Ti as well as a significant enrichment in the fluid mobile large ion lithophile elements (LILE) Ba, Rb and K as well as Sr and Eu.

#### MELT SOURCE AND GEODYNAMIC IMPLICATIONS

Most Thetyan ophiolites display an evolution from MORB-like to island arc tholeiites and boninites, calcalkaline and alkaline magmatism (Hawkins, 1977; 2003; Stern and Bloomer, 1992; Dilek et al., 2007, 2009; Principi et al., 2004).

The relatively low PRIMA-normalized values of most trace elements and the rare earth pattern with  $La_n/Yb_n$  ratios <1 and low  $La_n/Sm_n$  (<0.7), as well as low  $K_2O$  < 1.0 wt% ratios indicate, that the studied gabbros derived from a mantle source which was depleted by previous melting episodes, i.e. a typical N-MORB situation (Schilling et al., 1983). The heavy rare earth elements are more than four times enriched, indicating the lack of residual garnet in the mantle source and pointing to melt generation in the uppermost spinel-bearing mantle, too. The positive Eu anomaly point to unfractionated Ca-rich

Table 4. Chemical composition of amphiboles. Amphibole calculation based on 23 oxygens with Fe<sup>2+</sup>/Fe<sup>3+</sup> estimation assuming Σ13 cations B except for Fe, Mg, Mn amphiboles where Σ15 is applied. Classification after Leake et al. (1997), Leake (2004).

wt%	GI3	GI3	GI3	GI3	GI3	GI3	GI2	GI2	GI2	GI2	GI2
	rim	core	rim	core	rim	rim	rim cpx	rim cpx	rim cpx	rim cpx	rim cpx
SiO <sub>2</sub>	54.89	58.08	53.14	52.84	54.90	52.61	44.72	42.12	44.61	44.92	46.02
TiO <sub>2</sub>	0.20	0.17	0.20	0.28	0.14	0.04	1.54	3.64	2.77	2.31	2.06
Cr <sub>2</sub> O <sub>3</sub>	n.d.	n.d.	n.d.	0.12	n.d.	n.d.	n.d.	n.d.	0.03	n.d.	0.01
Al <sub>2</sub> O <sub>3</sub>	4.01	1.06	5.12	5.90	3.64	6.19	11.10	11.57	9.74	8.93	8.81
FeO	10.49	10.34	12.92	10.67	10.86	10.77	12.86	14.46	13.16	16.16	14.93
MnO	0.45	0.41	0.31	0.00	0.24	0.28	0.26	0.26	0.24	0.30	0.24
MgO	15.92	16.22	14.27	17.49	15.35	14.55	14.07	11.86	13.60	12.58	12.74
CaO	11.69	11.79	11.55	10.44	12.43	12.73	10.93	10.87	10.90	10.23	10.85
Na <sub>2</sub> O	0.38	n.d.	0.47	0.25	0.43	0.80	3.16	3.42	3.19	2.92	2.55
K <sub>2</sub> O	n.d.	n.d.	0.02	0.01	0.01	0.03	0.28	0.37	0.37	0.48	0.39
Cl	n.d.	n.d.	n.d.	n.d.	n.d.	0.04	n.d.	n.d.	n.d.	n.d.	n.d.
Total	98.03	98.07	98.00	98.00	98.00	98.04	98.92	98.57	98.61	98.83	98.60
Si	7.70	8.14	7.54	7.25	7.78	7.49	6.46	6.22	6.50	6.59	6.72
AlIV	0.30	0.00	0.46	0.75	0.22	0.51	1.54	1.78	1.49	1.40	1.27
AlVI	0.37	0.17	0.39	0.21	0.39	0.53	0.35	0.23	0.18	0.13	0.24
Ti	0.02	0.02	0.02	0.03	0.01	0.00	0.16	0.40	0.30	0.25	0.22
Cr	0.00	0.00	0.00	0.01	0.00	0.00	0.00	0.00	0.00	0.00	0.00
Fe <sup>3+</sup>	0.27	0.00	0.38	1.23	0.00	0.00	0.24	0.11	0.14	0.28	0.17
Fe <sup>2+</sup>	0.96	1.21	1.15	0.00	1.29	1.28	1.20	1.63	1.40	1.56	1.57
Mn	0.05	0.05	0.04	0.00	0.03	0.03	0.03	0.03	0.03	0.03	0.03
Mg	3.33	3.39	3.02	3.58	3.24	3.09	3.03	2.61	2.95	2.75	2.77
Ca	1.76	1.77	1.76	1.54	1.89	1.94	1.69	1.72	1.70	1.60	1.69
Na	0.10	0.00	0.13	0.07	0.12	0.22	0.16	0.21	0.21	0.22	0.19
K	0.00	0.00	0.00	0.00	0.00	0.01	0.05	0.07	0.07	0.09	0.52
Cl	0.00	0.00	0.00	0.00	0.00	0.01	0.00	0.00	0.00	0.00	0.00
Total	14.86	14.75	14.89	14.67	14.97	15.11	14.91	15.01	14.97	14.9	15.39
Species	actinolite	actinolite	actinolite	tremolitic hornblende	actinolite	actinolitic hornblende	pargasite	Ti-rich pargasite	Ti-rich pargasite	magnesio- hastingsite	pargasite

plagioclase, i.e. Ca<sup>2+</sup> substitution in a reducing magma in the early fractionation process (Atwood, 2012). The lack of quartz-normative samples is probably due to the low PH<sub>2</sub>O conditions of the melt source (Chayes, 1972). This point to a MORB generating flat source, too (Chayes, 1972; Kay, 1980). However, the depletion of the high field strength elements (HFSE) Nb, Zr, Ti, and Ta as well as P point to a mantle source influenced by subduction related processes, such as dehydration or melting of the downgoing slab. In addition, the above cited significant enrichment of the large ion lithophile elements (LILE) is a further evidence of subduction related fluids originated

from the dehydration of a subducted (oceanic?) slab. This resembles an ophiolitic supra subduction Zone (SSZ) crust in embryonic arc fore-arc environment (Dilek et al., 2005), scenarios where seafloor spreading followed subduction. Alternatively, a back arc position is possible.

The up to 70 times PRIMA normalized enrichment of K, Rb; Ba and Sr and up to 5 times higher values than the N-MORB and very low high field strength elements Nb, Ta and Ti concentration (Figure 4) suggest an unusual N-MORB character. In addition, enriched (E-MORB) do not show this kind of depletion (Schilling et al., 1983). Furthermore, the samples are characterized by high LILE/

Table 5. Chemical composition of chlorites. Chlorite calculation based on 28 oxygens with Fe<sup>2+</sup>/Fe<sup>3+</sup> and OH calculated assuming full site occupancy.

wt%	GI3	GI3	GI3	GI2
SiO <sub>2</sub>	33.29	32.80	34.43	35.40
TiO <sub>2</sub>	n.d.	n.d.	n.d.	n.d.
Cr <sub>2</sub> O <sub>3</sub>	n.d.	n.d.	n.d.	n.d.
Al <sub>2</sub> O <sub>3</sub>	18.11	19.05	17.81	16.75
FeO	14.89	13.30	13.66	14.51
MnO	n.d.	n.d.	n.d.	n.d.
MgO	22.70	23.84	23.09	22.32
CaO	n.d.	n.d.	n.d.	n.d.
Na <sub>2</sub> O	n.d.	n.d.	n.d.	n.d.
K <sub>2</sub> O	n.d.	n.d.	n.d.	n.d.
Total	88.99	88.99	88.99	88.98
Si	6.38	6.24	6.52	6.71
AlIV	1.62	1.76	1.48	1.29
AlVI	2.50	2.55	2.54	2.50
Ti	0.00	0.00	0.00	0.00
Cr	0.00	0.00	0.00	0.00
Fe <sup>3+</sup>	0.49	0.44	0.60	0.68
Fe <sup>2+</sup>	1.89	1.67	1.57	1.62
Mn	0.00	0.00	0.00	0.00
Mg	6.48	6.76	6.52	6.31
Ca	0.00	0.00	0.00	0.00
Na	0.00	0.00	0.00	0.00
K	0.00	0.00	0.00	0.00
Total	19.36	19.42	19.23	19.11
Species	diabantite in cpx	diabantite	diabantite	diabantite

HFSE ratios like the Ba/Nb ratio (Figure 4a). This reflects a significant crustal contamination of the source, whereas the low TiO<sub>2</sub> concentration display that Ti is available only in low concentrations. Jacques et al. (2013) and Wehrmann et al. (2014) show by comparing the composition of the rocks of the South American magmatic arc that the sediments from the Nazca Plate which are subducted at the trenches show a clear compositional relationship between subducted sediments and arc rocks. The high Ba/Nb ratios of the subducted sediments correlate with the high Ba/Nb ratios of the arc magmatism. The low Ti concentrations are a further evidence for a subduction zone influenced magma source (Figure 5b; Verma, 2006). Figure 5 shows the different contributions of mantle, island arc and/or

crustal components on melt composition. In Figure 5a the Timpa delle Murge samples reveal the strong crustal influence. Figure 5b compares the analyzed gabbros with N-MORB and other oceanic crustal compositions. The (La/Sm)<sub>n</sub> ratios and TiO<sub>2</sub> concentrations show weak similarities to Tonga-Kermadec arc environments (Figure 5b). Furthermore, the Sr/Ce ratio is a useful indicator of subduction derived fluids. According to Wehrmann et al. (2014 and references herein). Values over 50 (the analyzed samples ranges 70 to 150) indicate a strong contribution of subduction derived fluids, comparable to the arc rocks of Nicaragua. In contrast the comparable low LREE elements are indicator of the small contamination by crustal melts. The high Sr concentration shows a possible



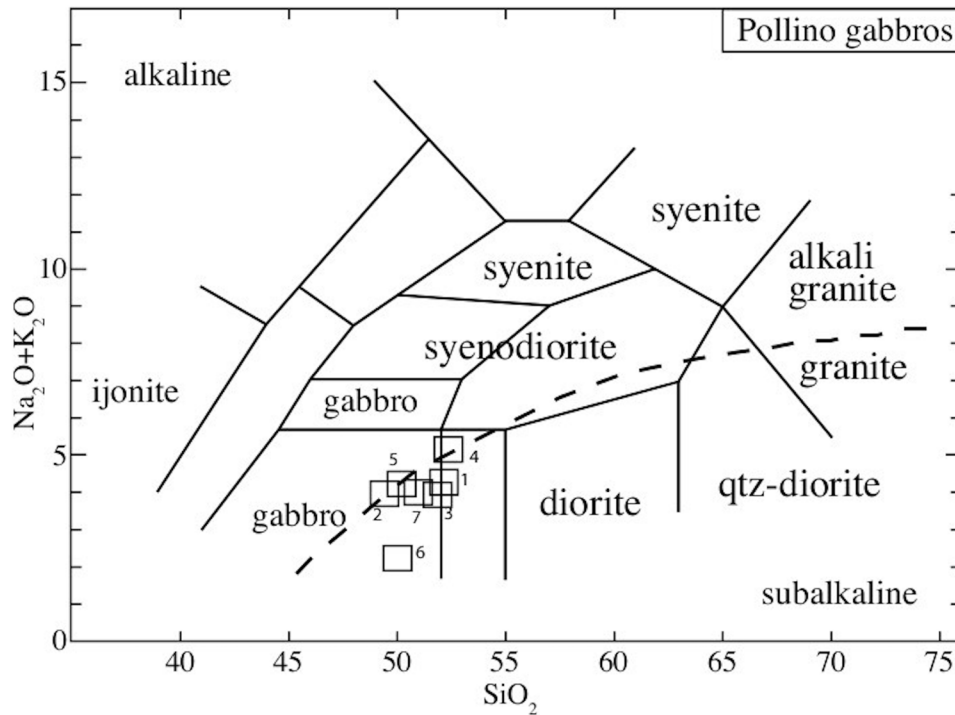


Figure 3. Total alkali versus  $\text{SiO}_2$  diagram after Le Bas et al. (1986).

additional seawater dehydration of the subducted plate.

In summary, the analyzed and discussed samples of the gabbros of the Timpa delle Murge ophiolite show evidence of a strong crustal component in an N-MORB – like melt. This interference is typical for mantle regions, which are influenced by subduction related fluids and episodic melting during mid-ocean-ridge processes.

Plausible localizations are oceanic back arc positions with embryonic MORB activities or fore arcs. Alternatively, recent studies at the Izu-Bonin-Mariana island arc, formed in a supra subduction zone environment, show similar slab contaminated magmatism in the early stage of the island arc formation (Ishizuka et al., 2014).

Similarities with Timpa delle Murge ophiolite, Izu-Bonin-Mariana and Tonga-Kermadec arc-trench (Dilek and Furnes, 2014) are shown in the Albanide-Hellenide ophiolites. These are in close association of MORB, IAT, boninites and MORB/IAT basalts (Beccaluva et al., 2005). This is related to distinctly different magma sources were contemporaneously active in a relatively restricted sector across an intraoceanic supra-subduction zone (SSZ) (Beccaluva et al., 2005).

The Internal Ligurides ophiolites are different from Timpa delle Murge. These ophiolites formed by intrusion of N-MORB type melts into a heterogeneous mantle (Tribuzio et al., 2004) and are similar to residual abyssal peridotites (Tribuzio et al., 2004). In particular, these were

subjected to different processes after the partial melting event, furthermore are isotopically depleted relative to associated crustal rocks, similar to what is observed for the modern oceanic lithosphere (Tribuzio et al., 2004).

## CONCLUSIONS

Timpa delle Murge and Albanide-Hellenide ophiolites can be classified as subduction-related (Dilek and Furnes, 2014), Internal Ligurides ophiolites as subduction-unrelated types (Dilek and Furnes, 2014).

An oceanic back arc system is generally formed by the subduction of an oceanic plate at an oceanic-oceanic convergent plate boundary. The geochemical features of back arc basin will vary with the development of spreading during initial stage back arc formation, and the late stage geochemical of mid-ocean ridge basalt (MORB) formation. Thus, geochemical signatures show MORB evidence with the development of a back arc basin and with the signatures being controlled by the interaction between the mantle components and the subduction zone components. Therefore, the present work indicates that the gabbros in the southern Apennines ophiolite have a clear back arc basin affinity. In particular, the gabbros in the Pollino area are plotted predominantly in the MORB field. This may imply that the gabbro in the Pollino area may be formed during the initiation of rifting. Recent geological and geophysical surveys in the Izu-Bonin-Mariana

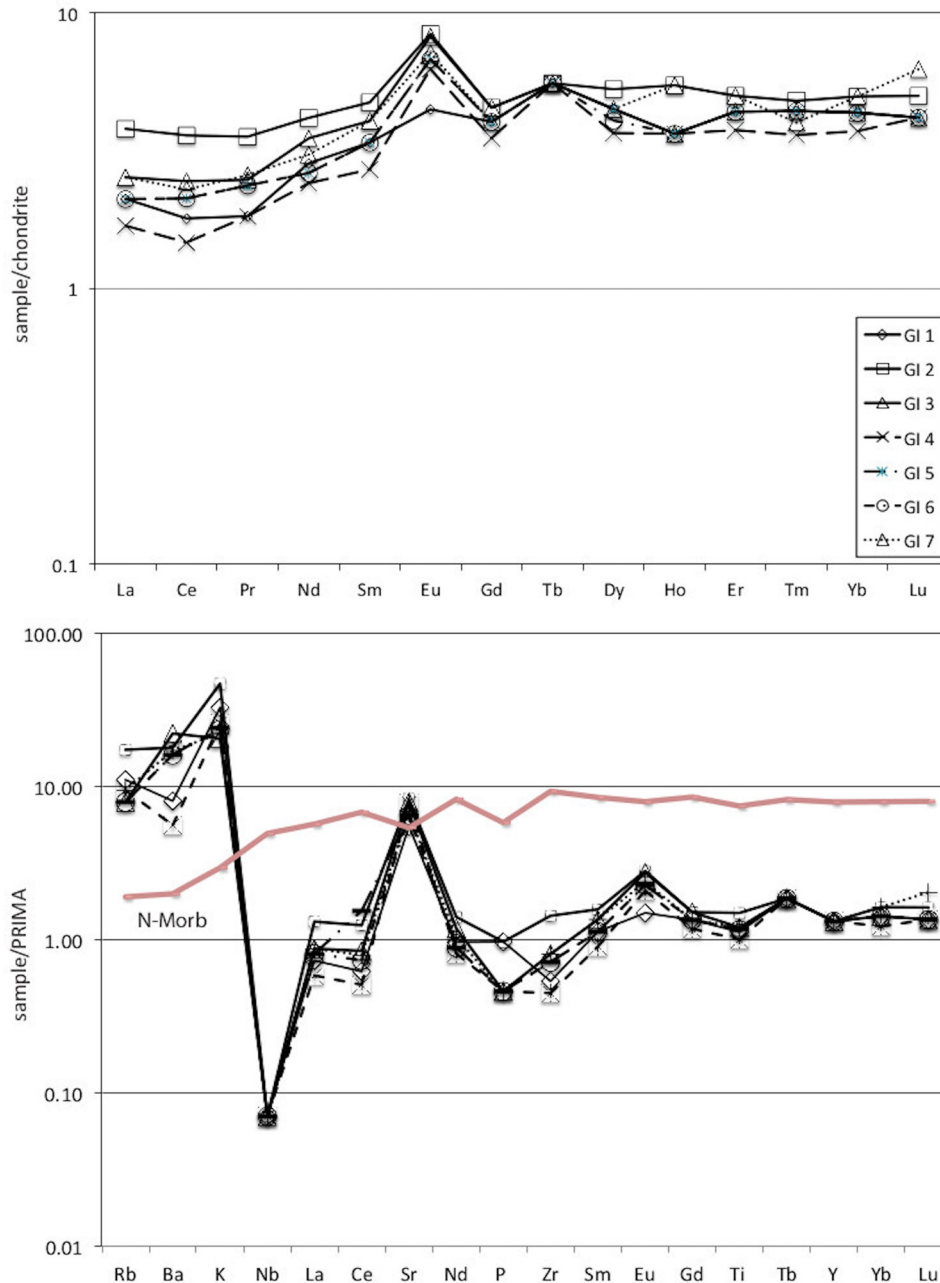


Figure 4. a) Chondrite normalized concentrations of the Rare Earth Elements. b) Primitive mantle normalized concentrations (after Sun and McDonough, 1989) of incompatible elements, including N-MORB basalts (after Hofmann, 1988).

forearc have revealed the occurrence on the seafloor of oceanic crust generated in the initial stages of subduction and the earliest stage of island arc formation (Ishizuka, 2014). The earliest magmatism after subduction initiation generated forearc basalts, and subsequently, boninitic and tholeiitic to calc-alkaline lavas were produced (Ishizuka, 2014). This volcanic stratigraphy and its time-progressive development are analogous to those documented from

many suprasubduction zone ophiolites (Dilek and Furnes, 2014; Ishizuka, 2014).

#### ACKNOWLEDGEMENTS

The authors thanks L. Gaggero for their helpful comments. The authors benefited from finance support by University of Basilicata research funds. Thanks to Birgit Fabian for the support in creating the figures.

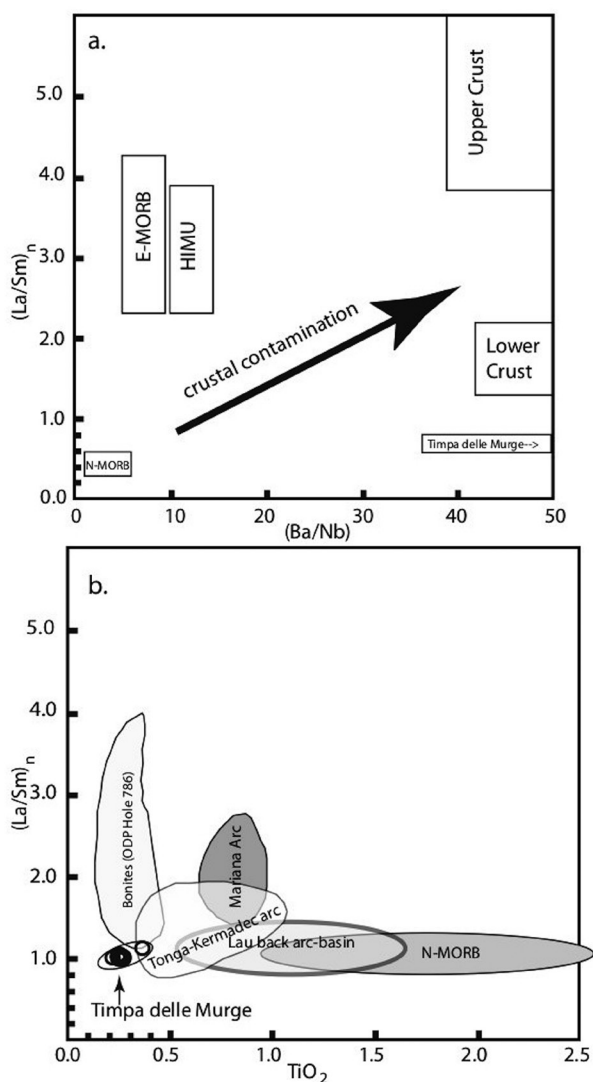


Figure 5. Comparison of the Timpa delle Murge samples and different melt influencing components or geodynamic settings. a)  $(La/Sm)_n$  vs.  $(Ba/Nb)$ . b)  $(La/Sm)_n$  vs.  $TiO_2$ . Compilation after Mattash et al. (2013) and Khanna (2013).

## REFERENCES

- Alt J.C., Shanks W.C., Crispini L., Gaggero L., Schwarzenbach E.M., Früh-Green G., Bernasconi S., 2012. Uptake of carbon and sulfur during seafloor serpentinization and the effects of subduction metamorphism in Ligurian peridotites. *Chemical Geology* 323, 268-277.
- Atwood D.A., 2012. *The Rare Earth Elements: Fundamentals and Applications*. Wiley, New York, 624 pp.
- Bebien J., Dimo-Lahitte A., Vergely P., Inser Gueix-Filippi D., Dupeyrat L., 2000. Albanian Ophiolites. I - magmatic and metamorphic processes associated with the initiation of a subduction. *Ophiolite* 25, 47-53.
- Beccaluva L., Maciotta G., Spadea P., 1982. Petrology and geodynamic significance of the Calabria-Lucania ophiolites. *Rendiconti Società Italiana di Mineralogia e Petrologia* 38, 973-987.
- Beccaluva L., Coltorti M., Saccani E., Siena F., 2005. Magma generation and crustal accretion as evidenced by supra-subduction ophiolites of the Albanide-Hellenide Subpelagionian zone. *The Island Arc* 14, 551-563.
- Bonardi G., Amore F.O., Ciampo G., De Capoa P., Miconnet P., Perrone V., 1988. Il Complesso Liguride Auct.: Stato delle conoscenze attuali e problemi aperti sulla sua evoluzione Pre-Appenninica ed i suoi rapporti con l'Arco Calabro. *Memorie della Società Geologica Italiana* 41, 17-35.
- Bonardi G., Ciarcia S., Di Nocera S., Matano F., Sgrosso I., Torre M., 2009. Carta delle principali Unità cinematiche dell'Appennino meridionale. Note illustrative. *Italian Journal of Geosciences* 128, 47-60.
- Bracciali L., Marroni M., Pandolfi L., Rocchi S., 2007. Geochemistry and petrography of Western Tethys Cretaceous sedimentary covers (Corsica and Northern Apennines): From source areas to configuration of margins. *Geological Society of America Special Papers* 420, 73-93.
- Cello G. and Mazzoli S., 1999. Apennine tectonics in southern Italy a review. *Journal of Geodynamics* 27, 191-211.
- Chayes S.F., 1972. Silica saturation in Cenozoic basalt. *Philosophical Transactions of the Royal Society of London. Ser. A* 271, 285-296 pp.
- Dichicco M.C., Laurita S., Paternoster M., Rizzo G., Sinisi R., Mongelli G., 2015. Serpentinite Carbonation for CO<sub>2</sub> Sequestration in the Southern Apennines: Preliminary Study. *Energy Procedia* 76, 477-486.
- Dichicco M.C., De Bonis A., Mongelli G., Rizzo G., Sinisi R., 2017.  $\mu$ -Raman spectroscopy and X-ray diffraction of asbestos' minerals for geo-environmental monitoring: The case of the southern Apennines natural sources. *Applied Clay Science* 141, 292-299.
- Dilek Y., Shallo M., Furnes H., 2005. Rift-drift seafloor spreading, and subduction zone tectonics of Albanian ophiolites. *International Geology Review* 47, 147-176.
- Dilek Y., Furnes H., Shallo M., 2007. Supra subduction zone ophiolite formation along the periphery of Mesozoic Gondwana. *Gondwana Research* 11, 453-475.
- Dilek Y. and Furnes H., 2009. Structure and geochemistry of Tethyan ophiolites and their petrogenesis in subduction rollback systems. *Lithos* 113, 1-20.
- Dilek Y. and Furnes H., 2014. Ophiolites and their origins. *Elements* 10, 93-100.
- Dogliani C., Gueguen E., Harabaglia P., Mongelli F., 1999. On the origin of west-directed subduction zones and applications to the western Mediterranean. *The Mediterranean basins: Tertiary extension within the alpine orogeny*. (eds): B. Durand, L. Jolivet, F. Horvát and M. Séranne, Special Publications Geological Society, London, 541-561.

- Franzini M., Leoni L., Saitta M., 1972. A simple method to evaluate the matrix effects in X-ray fluorescence analysis. *X-Ray Spectrom* 1, 151-154.
- Franzini M., Leoni L., Saitta M., 1975. Revisione di una metodologia analitica di fluorescenza-X basata sulla correzione completa degli effetti di matrice. *Rendiconti Società Italiana di Mineralogia e Petrologia* 31, 365-378.
- Giano S.I. and Giannandrea P., 2014. Late Pleistocene differential uplift inferred from the analysis of fluvial terraces (southern Apennines, Italy). *Geomorphology* 217, 89-105.
- Giano S.I., Gioia D., Schiattarella M., 2014. Morphotectonic evolution of connected intermontane basins from the southern Apennines, Italy: the legacy of the pre-existing structurally-controlled landscape. *Rend. Fis. Acc. Lincei* 25, 241-252.
- Gueguen E., Doglioni C., Fernandez M., 1998. On the post 25 Ma geodynamic evolution of the western Mediterranean. *Tectonophysics* 298, 259-269.
- Hawkins J.W., 1977. Petrological and geochemical characteristics of marginal basin basalts. *Island Arcs, Deep Sea Trench and back Arc Basins* (eds): M. Talwani, W.C. Pitman, American Geophysical Union, Washington, D.C., 355-365.
- Hofmann A.W., 1988. Chemical differentiation of the Earth: the relationship between mantle, continental crust, and oceanic crust. *Earth and Planetary Science Letters* 90, 297-314.
- Hawkins J.W., 2003. Geology of suprasubduction zones-implications for the origin of ophiolites. *Ophiolite Concept and the Evolution of Geological Thought*. (eds): Y. Dilek, S. Newcomb, Geological Society of America, Special Paper, 227-268.
- Hoeck V., Koller F., Meisel T., Onuzi K., Kneringer E., 2002. The Jurassic South Albanian ophiolites: MOR- vs. SSZ-type ophiolites. *Lithos* 65, 143-164.
- Insergueix-Filippi D., Dupeyrat T L., Dimo-Lahitte A., Vergely P., Bébien J., 2000. Albanian ophiolites. II - Model of subduction zone infancy at a mid- ocean ridge. *Ofioliti* 25, 47-53.
- Ishizuka O., Tani K., Reagan M.K., 2014. Izu-Bonin-Mariana Forearc Crust as a Modern Ophiolite Analogue. *Elements* 10, 115-120.
- Jacques G., Hoernle K., Gill J., Hauff F., Wehrmann H., Garbeb Schonberg D., Van Den Bogaard P., Bindeman I., Lara L.E., 2013. Across-arc geochemical variations in the Southern Volcanic Zone, Chile (34.5–38.0-S): constraints on mantle wedge and input compositions. *Geochimica Cosmochimica Acta* 123, 218-243.
- Kay R.W., Hubbert J.J., Gast P.W., 1970. Chemical characteristics and origin of oceanic ridge volcanic rocks. *Journal of Geophysical Research* 75, 1585-1613.
- Khanna T.C., 2013. Geochemical evidence for a paired arc-back-arc association in the Neoproterozoic Gadwal greenstone belt eastern Dharwar craton, India. *Current Science India*, 632-640.
- Knott S.D., 1987. The Liguride Complex of Southern ItalyHa Cretaceous to Paleogene accretionary wedge. *Tectonophysics* 142, 217-226.
- Knott S.D., 1994. Structure, kinematics and metamorphism in the Liguride Complex, Southern Apennine, Italy. *Journal of Structural Geology* 16, 1107-1120.
- Lagabriele Y. and Cannat M., 1990. Alpine Jurassic ophiolites resemble the modern central Atlantic basement. *Geology* 18, 319-322.
- Lanzafame G., Spadea P., Tortorici L., 1978. Provenienza ed evoluzione dei Flysch Cretacico-Eocenici della regione Calabro-Lucana. II: Relazioni tra ofioliti e Flysch Calabro-Lucano. *Ofioliti* 3, 189-210.
- Lanzafame G., Spadea P., Tortorici L., 1979. Mesozoic ophiolites of northern Calabria and Lucanian Apennine (Southern Italy). *Ofioliti* 4, 173-182.
- Laurita S., Prosser G., Rizzo G., Langone A., Tiepolo M., Laurita A., 2014. Geochronological study of zircons from continental crust rocks in the Frido Unit (Southern Apennines). *International Journal of Earth Sciences* 104, 179-203.
- Le Bas M.J., Le Maitre R.W., Streckeisen A., Zanettin B., 1986. A Chemical Classification of Volcanic Rocks Based on the Total-Alkali-Silica Diagram. *Journal of Petrology* 27, 745-750.
- Leake B.E., Whooley A.R., Arps C.E.S., Birch W.D., Gilbert M.S., Grise J.D., Hawthorne F.C., Kato K., Kish H.J., Krivovichev V.G., Linthout K., Laird J., 1997. Nomenclature of Amphiboles: Report of the Subcommittee on Amphiboles of the International Mineralogical Association, Commission on New Minerals and Mineral Names". *Canadian Mineralogist* 35, 219-246.
- Leake B.E., Whooley A.R., Birch W.D., Burke E.A.J., Ferraris G., Grise J.D., Hawthorne F.C., Kish H.J., Krivovichev V.G., Schumacher J.C., Stephenson N.C.N., Whittaker E.J.W., 2004. Nomenclature of amphiboles: Additions and revisions to the International Mineralogical Associations amphibole nomenclature. *American Mineralogist* 89, 883-887.
- Leoni L. and Saitta M., 1976. Determination of yttrium and niobium on standard silicate rocks by X-ray fluorescence analysis. *X-Ray Spectrom* 5, 29-30.
- Mattash M.A., Pinarelli L., Vaselli O., Minissale A., Albkadasi M., Shawki M.N., Tassi, F., 2013. Continental Flood Basalts and Rifting: Geochemistry of Cenozoic Yemen Volcanic Province. *International Journal of Geoscience* 10, 1453-1466.
- Menna F., 2009. From magmatic to metamorphic deformation in a Jurassic Ophiolitic Complex: the Bracco Gabbroic Massif, Eastern Liguria (Italy). *Ofioliti* 34, 109-130.
- Middlemost E.A.K., 1975. The basalt clan. *Earth Science Reviews* 11, 337-364.
- Monaco C., 1993. Le Unità Liguridi nel confine Calabro-Lucano (Appennino Meridionale): Controllo dei dati esistenti, nuovi dati ed interpretazione. *Bollettino Società Geologica Italiana* 112, 751-769.
- Monaco C. and Tortorici L., 1995. Tectonic role of ophiolite-



- bearing terranes in building of the Southern Apennines orogenic belt. *Terra Nova* 7, 153-160.
- Monaco C., Tansi C., Tortorici L., De Francesco A.M., Morten L., 1991. Analisi geologico-strutturale dell'Unità del Frido al confine calabro-lucano (Appennino Meridionale). *Memorie della Società Geologica Italiana* 47, 341-353.
- Monaco C., Tortorici L., Morten L., Critelli S., Tansi C., 1995. Geologia del versante Nord-Orientale del Massiccio del Pollino (Confine Calabro Lucano): Nota illustrativa sintetica alla scala 1:50,000. *Bollettino Società Geologica Italiana* 114, 277-291.
- Ogniben L., 1969. Schema introduttivo alla geologia del confine calabro-lucano. *Memorie della Società Geologica Italiana* 8, 453-763.
- Patacca E. and Scandone P., 2007. Geology of the southern Apennines. *Bollettino Società Geologica Italiana*, Special Issue 75-119.
- Pearce J.A., 2014. Immobile element fingerprinting of ophiolites. *Elements* 10, 101-108.
- Principi G., Bortolotti V., Chiari M., Cortesogno L., Gaggero L., Marcucci M., Cassani E., Treves B., 2004. The pre-orogenic volcano-sedimentary covers of the Western Tethys ocean basin: a review. *Ofioliti* 29, 177-211.
- Rampone E., Hofmann A.W., Piccardo G.B., Vannucci R., Bottazzi P., Ottolini L., 1996. Trace element and isotope geochemistry of depleted peridotites from an N-MORB type ophiolite (Internal Liguride, N. Italy). *Contributions to Mineralogy and Petrology* 123, 61-76.
- Rampone E., Piccardo G.B., Vannucci R., Bottazzi P., 1997. Chemistry and origin of trapped melts in ophiolitic peridotites. *Geochimica et Cosmochimica Acta* 61, 4557-4569.
- Rampone E., Piccardo G.B., Hofmann A.W., 2008. Multi-stage melt-rock interaction in the Mt. Maggiore (Corsica, France) ophiolitic peridotites: microstructural and geochemical evidence. *Contributions to Mineralogy and Petrology* 156, 453-475.
- Rampone E., Hofmann A.W., Raczek I., 2009. Isotopic equilibrium between mantle peridotite and melt: evidence from the Corsica ophiolite. *Earth and Planetary Science Letters* 288, 601-610.
- Rampone E. and Hofmann A.W., 2012. A global overview of isotopic heterogeneities in the oceanic mantle. *Lithos* 148, 247-261.
- Rizzo G., Sansone M.T.C., Perri F., Laurita S., 2016. Mineralogy and petrology of the metasedimentary rocks from the Frido Unit (southern Apennines, Italy). *Periodico di Mineralogia* 85, 153-168.
- Sansone M.T.C., Rizzo G., Mongelli G., 2011. Petrochemical characterization of mafic rocks from Ligurian ophiolites, southern Apennines. *International Geology Review* 53, 130-156.
- Sansone M.T.C. and Rizzo G., 2012. Pumpellyite veins in the metadolerite of the Frido Unit (southern Apennines-Italy). *Periodico di Mineralogia* 81, 75-92.
- Sansone M.T.C., Prosser G., Rizzo G., Tartarotti P., 2012a. Spinel-peridotites of the Frido Unit ophiolites (southern Apennines-Italy): evidence for oceanic evolution. *Periodico di Mineralogia* 81, 35-59.
- Sansone M.T.C., Tartarotti P., Prosser G., Rizzo G., 2012b. From ocean to subduction: the polyphase metamorphic evolution of the Frido unit metadolerite dykes (southern Apennine, Italy). Multiscale structural analysis devoted to the reconstruction of tectonic trajectories in active margins. (eds): G. Gosso, M.I. Spalla and M. Zucali, *Journal Virtual Explorer*, Electronic Edition, published online. ISSN: 1441B8142.
- Sanfilippo A. and Tribuzio R., 2011. Melt transport and deformation history in a nonvolcanic ophiolitic section, northern Apennines, Italy: Implications for crustal accretion at slow spreading settings. *Geochemistry Geophysics Geosystems* 12, 1-34.
- Sanfilippo A. and Tribuzio R., 2013. Building of the deepest crust at a fossil slow-spreading centre (Pineto gabbroic sequence, Alpine Jurassic ophiolites). *Contributions Mineralogy and Petrology* 165, 705-721.
- Schettino A. and Turco E., 2011. Tectonic history of the western Tethys since the Late Triassic. *Bulletin of the Geological Society of America* 123, 89-105.
- Schwarzenbach E., Früh-Green G.L., Bernasconi S.M., Alt J.C., Shanks W.C., Gaggero L., Crispini L., 2012. Sulfur geochemistry of peridotite-hosted hydrothermal systems: comparing the Ligurian ophiolites with oceanic serpentinites. *Geochimica et Cosmochimica Acta* 91, 283-305.
- Schiattarella M., 1996. Tettonica della Catena del Pollino (confine calabro-lucano). *Memorie della Società Geologica Italiana* 51, 543-566.
- Schilling J.G., Zajac M., Evans R., Johnston T., White W., Devine J.D., Kingsley R., 1983. Petrologic and geochemical variations along the Mid-Atlantic Ridge from 29°N to 73°N. *American Journal of Science* 283, 510-586.
- Spadea P., 1979. Contributo alla conoscenza dei metabasalti ofiolitici della Calabria Settentrionale e Centrale e dell'Appennino Lucano. *Rendiconti della Società Italiana di Mineralogia Petrologia* 35, 251-276.
- Spadea P., 1982. Continental crust rock associated with ophiolites in Lucanian Apennine (Southern Italy). *Ofioliti* 7, 501-522.
- Spadea P., 1994. Calabria-Lucania ophiolites. *Bollettino di Geofisica Teorica e Applicata* 36, 271-281.
- Stampfli G.M., Borel G.D., Marchant R., Mosar J., 2002. Western Alps geological constraints on western Tethyan reconstructions. Reconstruction of the evolution of the Alpine-Himalayan Orogen. (eds): G. Rosembaum, and G.S. Lister, *Journal of Virtual Explorer*, 77-106.
- Stern R.J. and Bloomer S.H., 1992. Subduction zone infancy: examples from the Eocene Izu-Bonin-Mariana and Jurassic California. *Geological Society of American Bulletin* 104,

1621-1636.

- Sun S.S. and McDonough W.F., 1989. Chemical and Isotopic Systematics of Oceanic Basalts: Implications for Mantle Composition and Processes. *Magmatism in the Ocean Basins* (eds): A. D. Saunders and M. J. Norry, Geological Society of London, Special Publication, 313-345.
- Tortorici L., Catalano S., Monaco C., 2009. Ophiolite-bearing mélanges in southern Italy. *Journal of Geology* 44, 153-166.
- Tribuzio R., Riccardi M.P., Ottolini L., 1995. Trace element redistribution in high temperature deformed gabbros from East Ligurian ophiolites (northern Apennines, Italy): Constraints on the origin of syndeformation fluids. *Journal of Metamorphic Geology* 13, 367-377.
- Tribuzio R., Tiepolo M., Vannucci R., Bottazzi P., 1999. Trace element distribution within the olivine-bearing gabbros from the Northern Apennine ophiolites (Italy): evidence for post-cumulus crystallization in MOR-type gabbroic rocks. *Contribution Mineralogy and Petrology* 134, 123-133.
- Tribuzio R., Thirwall M.F., Vannucci R., 2004. Origin of the gabbro-peridotite association from the Northern Apennine ophiolites (Italy). *Journal of Petrology* 45, 1109-1124.
- Verma S.P., 2006. Extension related origin of magmas from a garnet bearing source in the Los Tuxtlas volcanic field, Mexico. *International Journal of Earth Sciences* 95, 871-901.
- Vezzani L., 1969. La Formazione del Frido (Neocomiano Aptiano) tra il Pollino ed il Sinni. *Geologica Romana* 8, 129-176.
- Vezzani L., 1970. Le ofioliti della zona tra Castelluccio Inferiore e S. Severino Lucano (Potenza). *Atti della Accademia Gioenia di Scienze Naturali in Catania* 7, 1-49.
- Wehrmann H., Hoernle K., Garbebschönberg D., Guillaume J., Mahlke J., Schumann K., 2014. Insights from trace element geochemistry as to the roles of subduction zone geometry and subduction input on the chemistry of arc magmas. *International Journal of Earth Sciences* 103, 1929-1944.



This work is licensed under a Creative Commons Attribution 4.0 International License CC BY. To view a copy of this license, visit <http://creativecommons.org/licenses/by/4.0/>